APPLICATION OF WAVELET ANALYSIS TO ACOUSTIC EMISSION PULSES GENERATED BY ELECTRICAL DISCHARGES IN AIR

Tomasz Boczar
Technical University of Opole, Opole, Poland

Keywords: acoustic emission method, partial discharges, continuous and discrete wavelet transform, electrical discharges in the point-plane system in air

Abstract

The subject matter of this paper refers to the improvement of the acoustic emission (AE) method when used for detection, measurement and location of electrical discharges in air insulation systems of power appliances. The detailed subject matter refers to the issues connected with the application of modern methods of digital processing of signals obtained during technical high-power measurements. The paper presents the results of measurements and time-frequency analyses of the AE pulses generated by electrical discharges in the point-plane system in air. The AE pulses measured were subject to the wavelet analysis. For electrical discharges the continuous wavelet transform (CWT) was determined and the corresponding time-frequency distributions were drawn. Moreover, for the AE pulses generated by electrical discharges the discrete wavelet transform (DWT) was calculated, the runs of the particular details for seven frequency levels and the approximation run were presented. In reference to the DWT analysis for the particular details, the probability density functions (PDF) and the autocorrelation functions (ACF) were determined at the particular levels of decomposition. Also columnar diagrams showing the energy value that is transferred at the particular levels of decomposition were presented. Moreover, the energy density spectrum runs determined through a Fast Fourier Transform (FFT) were presented for comparison. The Morlet wavelet was used to determine the CWT, and the symlet wavelet was used to calculate the DWT. The acoustic pulses generated by electrical discharges in both positive and negative half-times of the voltage supplying the sparkgap under study were analyzed

1. Introduction

At present, the AE method enables detection, the measurement of intensity, and obtaining, in a limited range, information about the area of PD occurrence. A significant issue that occurs during the measurements taken on insulation systems of appliances operating in overhead power stations is eliminating interfering signals that can influence the results of the registered AE pulses generated by PDs. In industrial conditions the sources of interference can be physical phenomena caused by mechanical, electric or acoustic processes.

One of the possible sources of acoustic interference are corona, sliding and surface discharges, which can occur on the wires of overhead power lines, in stand-off and bushing insulators, and other appliances of power stations.

The aim of the research carried out, the results of which are presented in this paper, was registering and carrying out the time-frequency analysis using a short-time Fourier transform (STFT), a continuous and a discrete wavelet transforms of the AE pulses generated in the point-plane spark gap placed in air. Electrical discharges of this type can occur during PD measurements taken by using the AE method in industrial conditions. The AE signals generated by electrical discharges in air can disturb the measurements of PDs occurring in paper-oil insulation. Therefore the knowledge of interfering signals makes it possible to detect, and in consequence to eliminate them from the AE pulses generated by PDs occurring in insulation systems of power appliances. The information on time-frequency distributions will enable the selection of parameters of digital filters, which will make filtering of acoustic interfering signals from the measured AE pulses generated by PDs possible. This, in turn, can eliminate errors connected with the wrong interpretation of the measurement results obtained, and in consequence make the evaluation of the condition of the insulation measured more reliable.

2. Characteristics of the measuring apparatus used and the calculation procedures

For generation of electrical discharges in air a point-grounded plane spark gap was used, the electrodes of which were made of copper. The distance between the electrodes was 2 cm. The registration of the acoustic signals generated was carried out at the supplying voltage equal to 0.8 of the breakdown voltage of the system. The measuring transducer was 4 m away from the source of electrical discharges.

To measure acoustic interfering signals a standard system was used which is used for registration of the AE pulses generated by PDs. It consisted of the following items: a contact wideband piezoelectric transducer by the firm PAC of the series WD type AH-15, a NI-5911 measuring card by the National Instruments firm, and a measuring Nexus amplifier type 2692A-OS1 by the firm Brüel&Kjær. For the time-frequency analysis of the registered signals emitted by corona discharges were used: a short-time Fourier transform (STFT), a continuous wavelet transform (CWT), and a discrete wavelet transform (DWT). In order to visualize graphically the obtained results of the time-frequency transformations, amplitude spectrograms and power density spectra were used. The amplitude spectrograms were calculated as a module of the complex STFT, and the power density spectra were determined as a square of this module. Also scaling diagrams were drawn which were calculated as a square of the continuous wavelet transform (CWT) module, and the runs of the wavelet decomposition were determined for seven levels, which were calculated by using the discrete wavelet transform (DWT). For comparison the runs of the amplitude frequency spectra and the energy density spectra were drawn, which were calculated as a module and a square of the complex Fourier transform module, respectively. A detailed description of the formulae and calculation procedures used has been presented, among others, in the works [1, 2, 3].

3. The analysis of the results obtained

For the purpose of comparison Figs 1-4 show the results of the frequency analysis carried out by using the FFT for the AE pulses generated by sliding discharges in air, separately for the positive (Fig. 1-2) and negative voltage polarizations (Figs 3-4). Figs 1 and 3 illustrate amplitude spectrum distributions calculated as a module of the complex Fourier transform. Figs 2 and 4 show distributions of the energy density spectrum, which were determined as a square of the complex Fourier transform. Regardless of the supplying voltage polarization the frequency spectrum distributions were obtained which did not differ statistically, and the dominant frequency bands of which, read for the discrimination threshold -20dB, are within the ranges (30-60) kHz and (200-250) kHz.

Figs 5-10 show time-frequency distributions which were determined by using the STFT for the AE pulses generated by sliding discharges, separately for the positive (Figs 5-7) and negative (Figs 8-10) voltage halftimes. The two- and three-dimensional spectrograms presented in Figs 5-10 are of similar shapes of time-frequency distributions for both voltage polarizations. In the pictures obtained the same time-frequency structures can be observed, the noise signals, which occurred during the time of the whole acoustic event, for a given voltage polarization, in the following frequency bands: (30-50) kHz and (200-225) kHz. The use of the time-frequency analysis made it possible to identify the coherent structures, which occur in the time (1.5 – 2) ms, and with which the frequency band (30-350) kHz corresponds. There can be also observed time-frequency structures in the range (450-500) kHz at the positive voltage polarization and in the range (450-480) kHz for the negative voltage polarization. In these bands the size of the power transferred and the amplitude size of the AE pulses are about four times smaller than for the structures for low frequencies.

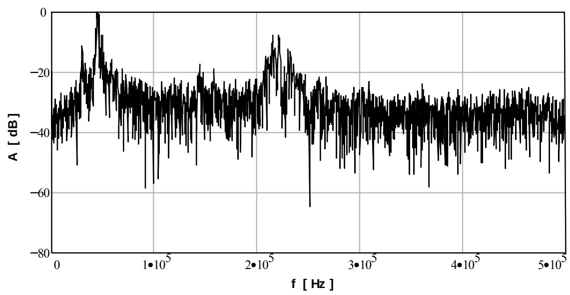

Figure 1: Amplitude spectrum run of the AE pulses generated by electrical discharges in the point-plane system in air, during the positive voltage half-period

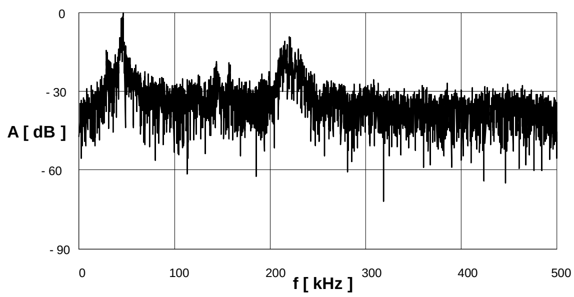

Figure 3: Amplitude spectrum run of the AE pulses generated by electrical discharges in the point-plane system in air, during the negative voltage half-period

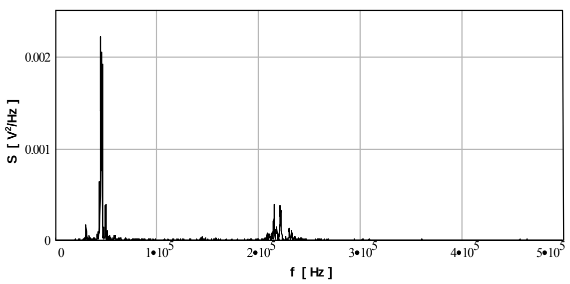

Figure 2: Energy density spectrum run of the AE pulses generated by electrical discharges in the point-plane system in air, during the positive voltage half-period

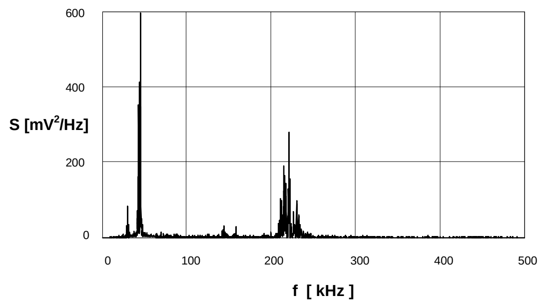

Figure 4: Energy density spectrum run of the AE pulses generated by electrical discharges in the point-plane system in air, during the negative positive voltage half-period

Figs 11-12 show time-frequency distributions calculated by using the CWT. Additionally, these figures show time runs of the AE pulses registered. For both voltage polarizations there occur coherent pictures in the band (30-60) kHz and in the range (200-500) kHz, but of almost three times lower power.

The results obtained by using the DWT are shown in Fig. 13 for the AE pulses generated by sliding discharges in air for the positive voltage polarization. Since for the negative voltage polarization the results of the wavelet decomposition obtained were the same, they have been neglected in this paper. The wavelet analysis was carried out for seven decomposition levels, and the particular details corresponded with the following frequency bands: D1 – (100-200) kHz …

Moreover, for the purpose of comparison, the runs of the probability density function – PDS (Fig. 14) and the autocovariance function (Fig. 15) were determined for the details analyzed. On the diagrams showing time runs obtained for the seven wavelet decomposition levels there can be observed active structures for details D1, D3, D4, D5. The runs of details D6 and D7, however, are of the noise signal character.

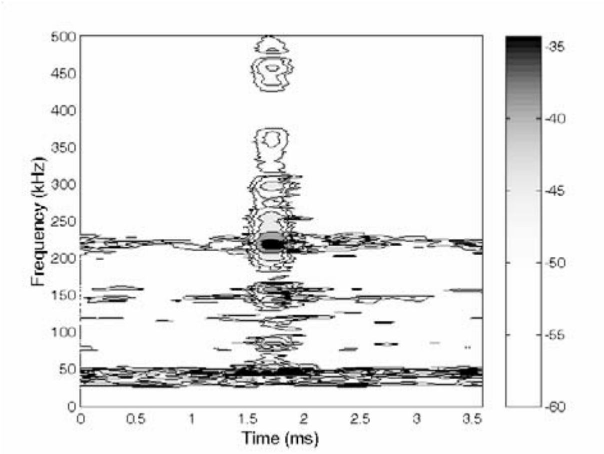

Figure 5: Spectrogram calculated for the AE pulses generated by electrical discharges in the point-plane system in air, during the positive voltage half-period

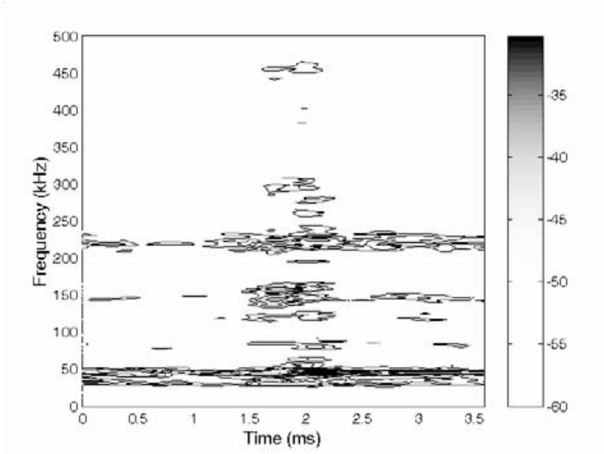

Figure 8: Spectrogram calculated for the AE pulses generated by electrical discharges in the point-plane system in air, during the negative voltage half-period

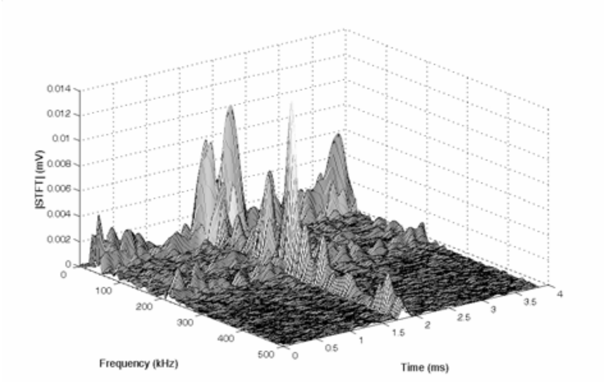

Figure 6: Three-dimensional spectrogram of power density spectrum of the AE pulses generated by electrical discharges in the point-plane system in air, during the positive voltage half-period

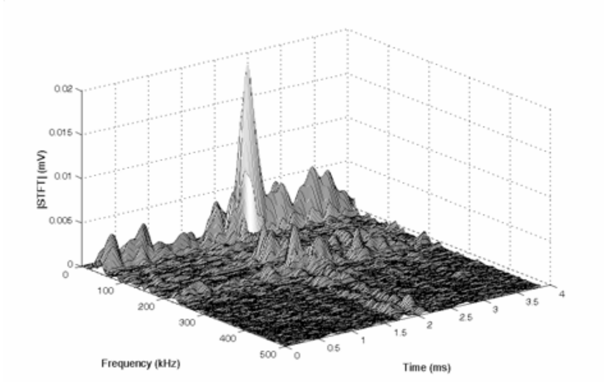

Figure 9: Three-dimensional spectrogram of power density spectrum of the AE pulses generated by electrical discharges in the point-plane system in air, during the negative voltage half-period

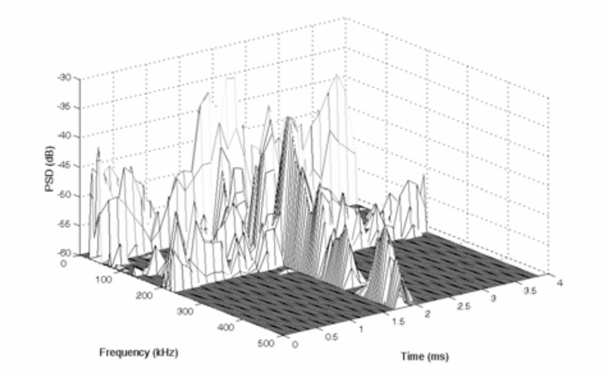

Figure 7: Three-dimensional spectrogram of amplitude spectrum calculated for AE pulses generated by electrical discharges in the point-plane system in air, during the positive voltage half-period

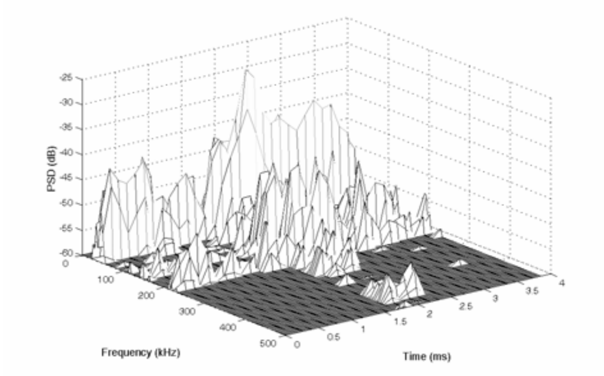

Figure 10: Three-dimensional spectrogram of amplitude spectrum calculated for AE pulses generated by electrical discharges in the point-plane system in air, during the negative voltage half-period

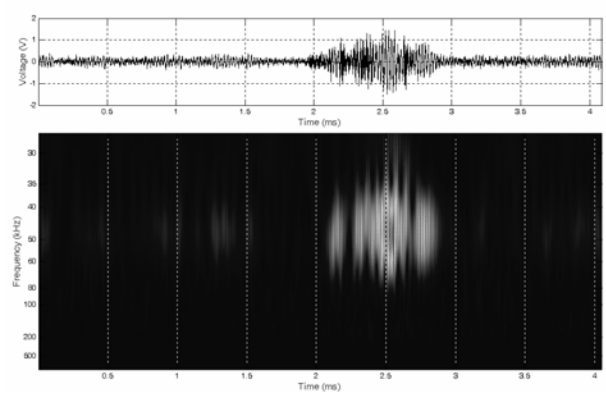

Figure 11: CWT of the AE pulses generated by electrical discharges in the point-plane system in air, during the positive voltage half-period

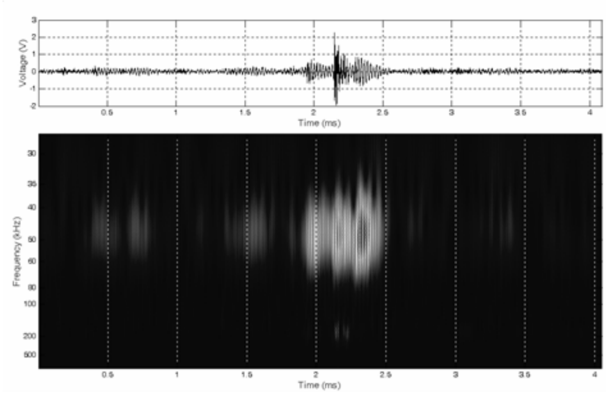

Figure 12: CWT of the AE pulses generated by electrical discharges in the point-plane system in air, during the negative voltage half-period

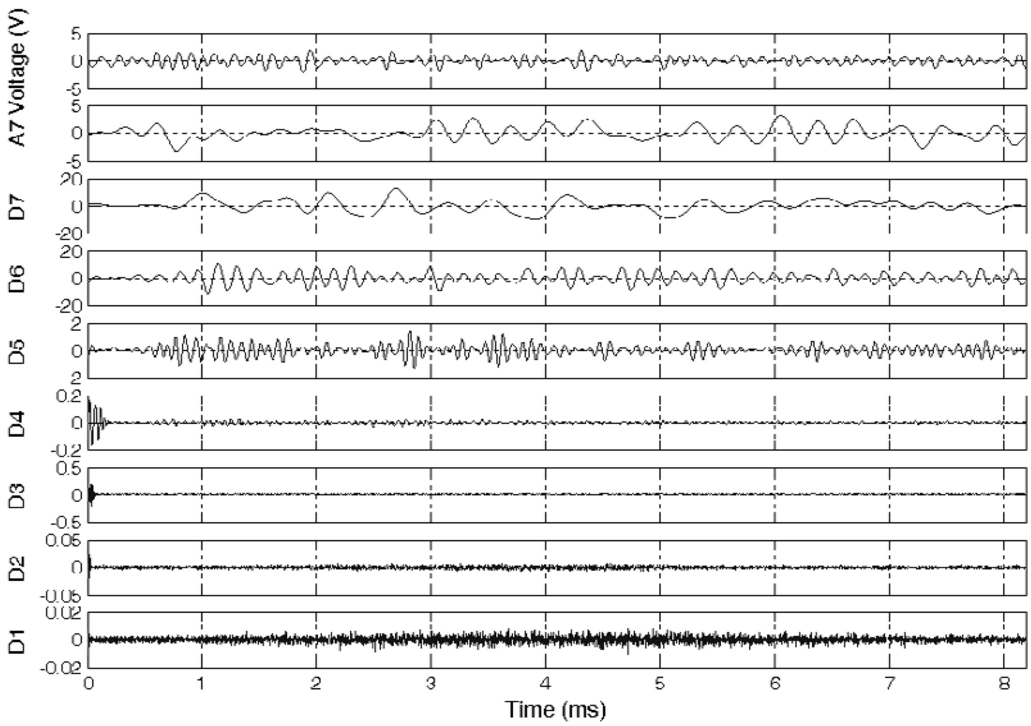

Figure 13: DWT of the AE pulses generated by electrical discharges in the point-plane system in air, during the positive voltage half-period

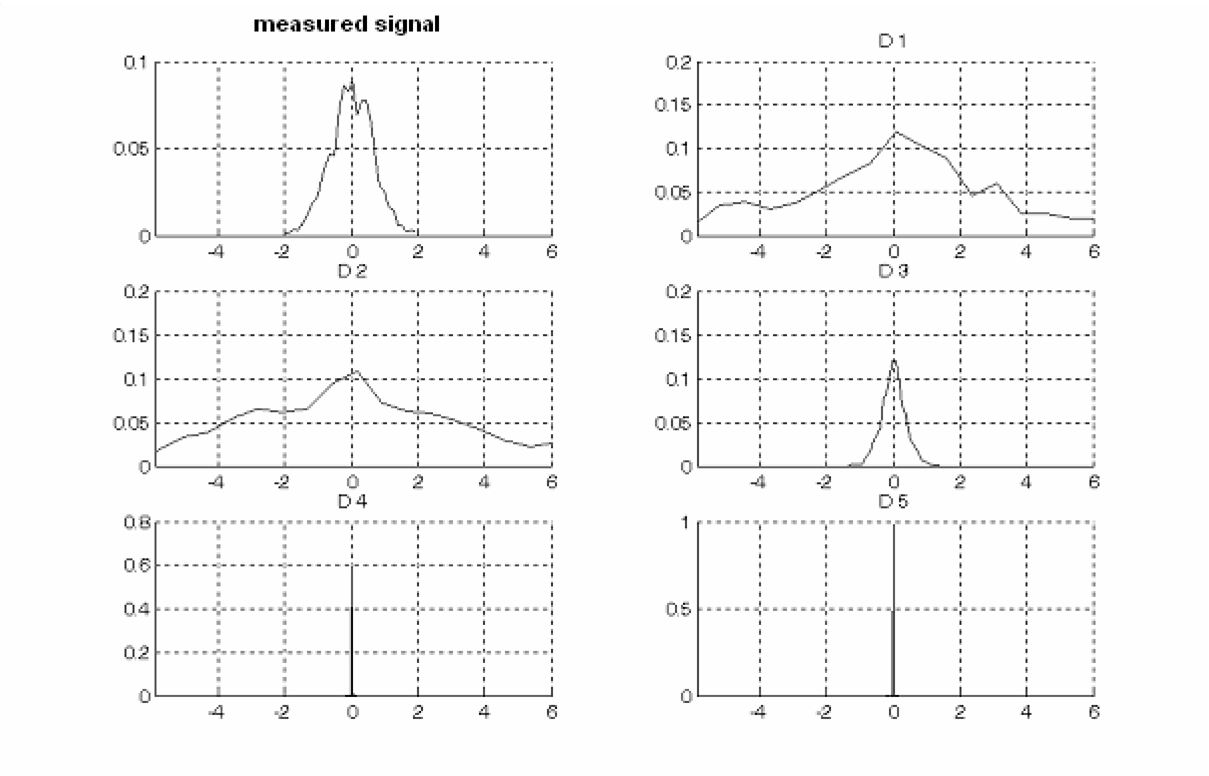

Figure 14: PDF of the AE pulses generated by electrical discharges in the point-plane system in air, during the positive voltage half-period

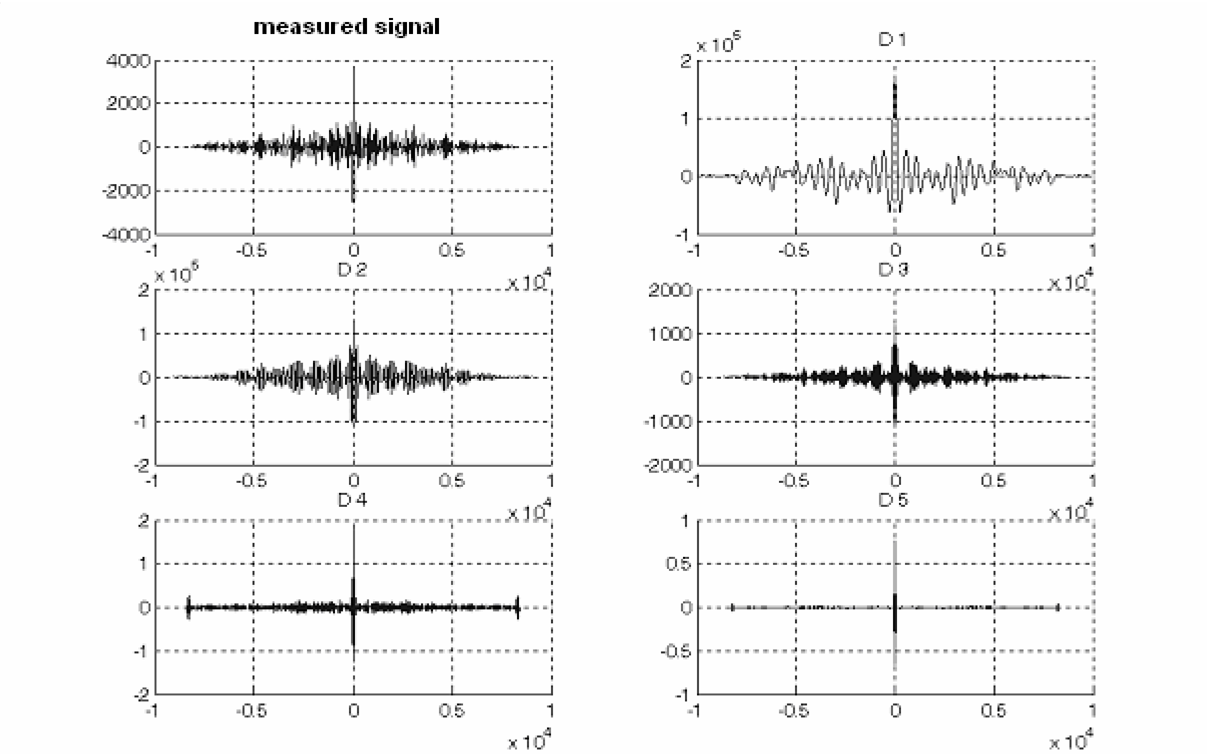

Figure 15: ACF of AE pulses generated by electrical discharges in the point-plane system in air, during the positive voltage half-period

Analyzing PDS runs for the particular details a varied degree of their slenderness can be observed. The biggest concentration was obtained for details D4 and D5, the shape of which is similar to that of the Dirac pulse. The PDS runs for details D1 and D2 are more flattened and the degree of their concentration smaller. For the signal measured and for detail D3 similar in shape PDS runs were obtained.

The autocovariance function makes it possible to determine the participation of stochastic and determining components in the AE pulses registered. For each detail and for the signal measured a big participation of the noise component can bee observed for a zero time shift. Moreover, for bigger time shifts there occur periodical components of varied amplitudes and quantities for the particular details and the signal measured. It points to a dual character of the registered AE pulses generated by sliding discharges in air where both noise and periodical components are the source of information on the acoustic event measured.

4. Conclusion

The application of time-frequency transformations, especially the analysis using continuous and discrete wavelet transforms, made it possible to isolate frequency bands of the noise signals from the time-frequency distributions determined, to associate frequency structures with the time of the AE pulse occurrence, and to determine the participation of the particular frequency components in the size of the energy transferred by the AE pulses measured.

The occurrence of electrical discharges in the point-plane system in air,on stand-off and bushing insulators is accompanied by the AE pulse generation, which can be the source of acoustic signals. These signals can disturb diagnostic measurements of PDs taken in industrial conditions using the AE method. Therefore, the knowledge of the time-frequency structure of the AE signals generated by electrical discharges in the point-plane system in air, will enable their effective filtration during the measurements of PDs occurring in insulation systems of power appliances. Moreover, the knowledge of the time-frequency structure of the AE signals generated by electrical discharges in the point-plane system in air,on the surface of insulators will enable a more effective comparison of various types of insulation materials and getting to know the mechanisms of occurrence and development of electrical discharges occurring on their surface.

References

[1] T. Boczar, „Frequency Analysis of Disturbing Signals Generated by Corona Discharges in Overhead Power Lines", The International Congress and Exhibition on Noise Control Engineering The Hague, The Netherlands, 2001, pp. 2191-94.

[2] T. Boczar , „Time-Frequency Analysis of Acoustic Emission Pulses Generated by Partial Discharges", *Journal of Electrical Engineering,* Bratislava, Slovakia, Vol. 54, No. 3-4, 2003, pp. 63-68.

[3] T. Boczar, D. Zmarzły, „Multiresolution Analysis of the Acoustic Emission Pulses Generated by Partial Discharges", *INSIGHT – The Journal of the British Institute of Non-Destructive Testing*, Vol. 45, No. 7, Great Britain, 2003, pp. 488-492.

The research was carried out within the grant KBN no. 4 T10A 019 25